Noncentrosymmetric far-zone spectral density induced by light scattering with random media having parity-time symmetry

Xuan Zhang,[1] Yonglei Liu,[2] Yahong Chen,[1,*] Fei Wang,[1,†] and Yangjian Cai[1,2,‡]

[1]*School of Physical Science and Technology, Soochow University, Suzhou 215006, China*

[2]*Shandong Provincial Engineering and Technical Center of Light Manipulation and Shandong Provincial Key Laboratory of Optics and Photonic Devices, School of Physics and Electronics, Shandong Normal University, Jinan 250014, China*

(Received 9 August 2021; revised 9 December 2021; accepted 2 February 2022; published 14 February 2022)

We study the scattering property of a normally incident plane wave scattered by random media whose second-order potential correlation function has parity-time ($\mathcal{PT}$) or classical symmetry. Based on the weak-potential-scattering theory, we show analytically that when the random media have classical symmetry, the far-zone spectral density is centrosymmetric. However, the spectral density becomes asymmetric for the $\mathcal{PT}$ random scatterer. The reason is the odd-symmetric distribution of the phase in the potential correlation function of the $\mathcal{PT}$ random media. We demonstrate numerically the asymmetric far-zone spectral density with two types of potential correlations, i.e., Schell-model-correlated and nonuniform-correlated correlations.

DOI: 10.1103/PhysRevA.105.023510

I. INTRODUCTION

Light scattering is one of the most common optical phenomena in nature and has become a basic subject in optics [1]. The intriguing physics behind it is promising for diverse applications, such as in optical imaging [2], optical trapping [3], crystallography [4], and atmospheric optics [5]. Due to the omnipresent random fluctuations in electromagnetic fields [6] and media [7], the effect of optical coherence on light scattering may not be ignored and, sometimes, plays a key role. Such a coherence effect may appear in two aspects of the light-scattering process. First, the incident light beam can be partially coherent [8]. Second, the scatterer medium is not always deterministic and can show randomness in its physical properties [9]. Extensive attention has been paid to the effect of the optical coherence of the incident beam on light scattering by deterministic media, including spherical scatterers [10–13], water droplets and ice crystals [14], inhomogeneous media [15], cylinders [16,17], and plasmonic nanostructures [18]. It has been shown that not only the spatial coherence width but also the spatial coherence structure of the incident beam has an impact on the scattered field. By engineering the spatial correlation of the incident partially coherent beam into the Bessel-correlated type, Wang *et al.* showed that in Mie scattering the far-zone directionality can be controlled and a conelike scattered field can be generated in the far field [19]. When the Bessel-correlated beam is scattered by a crystalline object, anomalous von Laue rings and ellipses can be created instead of the classic pointlike spots [20].

On the other hand, the scatterer medium, such as a fluid [6], turbulent atmosphere [5,21], dynamic ground glass [22], and even graphene samples [23,24], may exhibit random fluctuations in its physical properties. Such a random medium cannot be described by the deterministic potential function. Instead, its (second-order) statistical property is involved in the two-point potential correlation function (or matrix) [9]. The potential correlation function of the Gaussian Schell-model type has been considered in many circumstances [25]. The effect of the spatial coherence width of the potential correlation function on the near-field and far-field scattered fields has been studied [23,24,26–30]. The potential correlation function of the random medium can be inversely recovered from the measurement of the correlation function of the far-zone scattered field [31–33]. Recently, Korotkova and her colleagues showed that by shaping the potential correlation function into the non-Gaussian-correlated types, the scattered field can also be modulated, i.e., into the ringlike or rectangular scattered intensity patterns [34,35].

In this work, we study the scattering properties of the random media whose second-order potential correlation functions have parity-time ($\mathcal{PT}$) symmetry. We term such media the $\mathcal{PT}$ random media. $\mathcal{PT}$ random medium is an extension of a deterministic medium with the $\mathcal{PT}$-symmetric potential function, which was first introduced by Brandão and Korotkova [36]. The notion of $\mathcal{PT}$ symmetry was initially proposed in quantum mechanics that generalized the real Hermitian systems into the complex domain [37,38]. The first experimental observation of the $\mathcal{PT}$-symmetry-induced phenomena extended the study into the field of optics [39,40]. The $\mathcal{PT}$ symmetry in optics has found numerous applications, such as in unidirectional invisibility [41], anisotropic transmission resonances [42,43], single-particle detection [44], microlaser [45], lasers without inversion [46], robust wireless power transfer [47], and topological insulators [48]. The partially coherent Gaussian Schell-model beam scattered by $\mathcal{PT}$ deterministic media, such as two-point scatterers [49,50], localized continuous materials [51], and periodic materials [52]

*yahongchen@suda.edu.cn
†fwang@suda.edu.cn
‡yangjiancai@suda.edu.cn

with loss and gain, is studied. It has been shown that the non-Hermitian property of the scattering potential induces anomalous spectral changes in partially coherent scattered fields. More recently, Brandão and Korotkova introduced the concept of $\mathcal{PT}$ random media and gave a theoretical framework for the scattering of scalar radiation from the $\mathcal{PT}$ random media [36]. A detailed analysis of light scattering from the random $\mathcal{PT}$-symmetric particulate collections was given by the same authors [53].

Here, we examine the scattering properties of a normally incident plane-wave interaction with $\mathcal{PT}$ random media with the second-order potential correlation functions having Schell-model-correlated and nonuniformly correlated forms with the help of the first-order Born approximation (weak-potential-scattering theory) and the fundamental coherence theory. We show that the complex Schell-model-correlated potential correlations always display $\mathcal{PT}$ symmetry, while the nonuniformly correlated potential correlations show $\mathcal{PT}$ symmetry only when the phase of the correlation function is odd symmetric. We further show that $\mathcal{PT}$ symmetry embedded in the potential correlations will induce noncentrosymmetric distribution, while mirror symmetry (which we term classic symmetry in this work) induces centrosymmetric distribution, in the spectral density of the scattered field in the far zone. Our findings are expected to have use in determining the intrinsic symmetry properties of random materials.

We remark that the multiple scattering of a light wave in disordered media with loss or gain properties has been studied extensively with both classical and quantum approaches, which has led to a deeper understanding of the energy transport and strong localization effects of light in complex random media [54–60]. The results have led to applications in the visualization of the Anderson localization of light [61–64], random lasing [57,58,65,66], and light shaping through disordered photonic crystals [67–70]. In this work, we focus on light scattering within the first-order Born approximation; that is, the refractive index of the random medium differs only slightly from unity, and the scattering is weak. We aim to find out the effect of the potential correlation function's symmetry of the random scatterer on the far-field spectral density modulation.

This work is organized as follows. In Sec. II we examine the potential correlation functions for the $\mathcal{PT}$ random media with Schell-model-correlated and nonuniformly correlated correlations. In Sec. III we derive the analytical formulas for light scattering by the $\mathcal{PT}$ random media. In Sec. IV we give the simulation results for the far-zone spectral density induced by the normally incident plane-wave interaction with $\mathcal{PT}$ random media and reveal the noncentrosymmetric far-zone spectral density induced by the $\mathcal{PT}$-symmetric potential correlations. In Sec. V we summarize the main results of this work.

II. POTENTIAL CORRELATION FUNCTION OF $\mathcal{PT}$ RANDOM MEDIA

Due to the similar mathematical structures, under certain conditions, of the Schrödinger equation for electrons and Maxwell's theory of light, the complex potential in quantum mechanics can be viewed to be equivalent to a complex refractive index in optics [40]. Two opposite signs of the imaginary part of the refractive index represent the optical gain and loss in the material, respectively. When the gain and loss are equally balanced, i.e., the imaginary part of the refractive index is odd under inversion,

$$n''(-\mathbf{r}) = -n''(\mathbf{r}), \tag{1}$$

the material is a $\mathcal{PT}$-symmetric material. Above, the double prime denotes for the imaginary part. The real part of the refractive index of the $\mathcal{PT}$-symmetric material obeys $n'(-\mathbf{r}) = n'(\mathbf{r})$, where the prime denotes the real part. Thus, the complex refractive index for a $\mathcal{PT}$-symmetric material satisfies the condition

$$n(-\mathbf{r}) = n^*(\mathbf{r}), \tag{2}$$

where the asterisk stands for the complex conjugate. However, for a mirror-symmetric (classic-symmetric) material, the refractive index obeys the geometrical symmetry, i.e.,

$$n(-\mathbf{r}) = n(\mathbf{r}). \tag{3}$$

For a deterministic medium, its scattering potential V at position $\mathbf{r}$ and (angular) frequency ω has the following relation with the refractive index [9]:

$$V(\mathbf{r}, \omega) = \frac{k^2}{4\pi^2}[n^2(\mathbf{r}, \omega) - 1], \tag{4}$$

where $k = \omega/c$ is the wave number of the incident light, with c being the light speed in vacuum. Inserting the $\mathcal{PT}$-symmetric condition in Eq. (2) into (4), we find the complex potential function has a similar relation:

$$V(-\mathbf{r}, \omega) = V^*(\mathbf{r}, \omega). \tag{5}$$

For the classic-symmetric medium, its potential function $V(-\mathbf{r}, \omega) = V(\mathbf{r}, \omega)$.

We now take the potential function $V(\mathbf{r}, \omega)$ in Eq. (4) to represent a realization of a random medium, whereupon the (spectral) potential correlation function [6,8,9], characterizing all the second-order statistical properties of the random, statistically stationary medium, can be written as

$$C(\mathbf{r}_1, \mathbf{r}_2, \omega) = \langle V^*(\mathbf{r}_1, \omega)V(\mathbf{r}_2, \omega)\rangle_m, \tag{6}$$

where $\langle\cdot\rangle_m$ denotes the ensemble average over the medium realizations and $\mathbf{r}_1$ and $\mathbf{r}_2$ are two arbitrary position vectors within the scatterer volume. Inserting Eq. (5) into Eq. (6), we find that for a $\mathcal{PT}$ random medium the potential correlation function obeys

$$C(\mathbf{r}_1, \mathbf{r}_2, \omega) = C^*(-\mathbf{r}_1, -\mathbf{r}_2, \omega). \tag{7}$$

For a classic-symmetric medium, the relation $C(\mathbf{r}_1, \mathbf{r}_2, \omega) = C(-\mathbf{r}_1, -\mathbf{r}_2, \omega)$ holds.

To represent a genuine potential correlation function, it is sufficient to write $C(\mathbf{r}_1, \mathbf{r}_2, \omega)$ as [34,36]

$$C(\mathbf{r}_1, \mathbf{r}_2, \omega) = \int p(\mathbf{v})\mathcal{A}^*(\mathbf{r}_1, \mathbf{v})\mathcal{A}(\mathbf{r}_2, \mathbf{v})d^3\mathbf{v}, \tag{8}$$

where the spectral distribution $p(\mathbf{v})$ is a real, non-negative function, i.e., $p(\mathbf{v}) \geqslant 0$ and $p^*(\mathbf{v}) = p(\mathbf{v})$. $\{\mathcal{A}(\mathbf{r}, \mathbf{v})\}$ can be regarded as the generalized modes of the random scatterer potential corresponding to a continuous spectrum labeled by

the variable $\mathbf{v}$. For the $\mathcal{PT}$ random media, it is sufficient to have the condition

$$\mathcal{A}(-\mathbf{r}, \mathbf{v}) = \mathcal{A}^*(\mathbf{r}, \mathbf{v}), \tag{9}$$

which implies that the generalized modes are $\mathcal{PT}$ symmetric as well. However, for the classic-symmetric random media, no additional condition is imposed on the generalized modes since the relation $C(-\mathbf{r}_1, -\mathbf{r}_2, \omega) = C^*(\mathbf{r}_2, \mathbf{r}_1, \omega)$ always holds for the classic-symmetry random media. Above, we use the relation $C(\mathbf{r}_2, \mathbf{r}_1, \omega) = C^*(\mathbf{r}_1, \mathbf{r}_2, \omega)$, which is obtained by switching the order of spatial arguments in the complex-valued correlation function in Eq. (6).

$\mathcal{PT}$ random media with customized potential correlation functions can be accomplished with modern manufacturing techniques such as three-dimensional (3D) printing and can be realized by the 3D structure made with nested layers of liquid-crystal cells [34]. The engineered disordered 3D photonic structure or engineered disordered graphene layers could also be possible solutions for the experimental implementation of $\mathcal{PT}$ random media [71].

Next, we will introduce two kinds of potential correlation functions. One obeys the Schell-model type; that is, the (normalized) correlation function depends only on the position difference $\mathbf{r}_1 - \mathbf{r}_2$. The other one is the non-Schell-model type; that is, the spatial distribution of the correlation function is nonuniform. To simplify the calculation in Sec. III, we assume that the potential correlation functions in both cases are uncorrelated along the light-propagation direction (say, the z axis); thus, the potential correlation function can be written as

$$C(\mathbf{r}_1, \mathbf{r}_2, \omega) = C(\boldsymbol{\rho}_1, \boldsymbol{\rho}_2, \omega)\delta(z_1 - z_2), \tag{10}$$

where $\boldsymbol{\rho}_1 \equiv (x_1, y_1)$ and $\boldsymbol{\rho}_2 \equiv (x_2, y_2)$ are two arbitrary transverse position vectors and $\delta(\cdot)$ is a Dirac delta function.

A. Schell-model type

We now consider a famous class of correlation functions in which the degree of correlation [6] depends only on the position difference, i.e., $C(\mathbf{r}_1, \mathbf{r}_2, \omega) = [S(\mathbf{r}_1)S(\mathbf{r}_2)]^{1/2}F(\mathbf{r}_d, \omega)$, where $\mathbf{r}_d = \mathbf{r}_2 - \mathbf{r}_1$, $S(\mathbf{r})$ denotes the spectral density at position $\mathbf{r}$, and $F(\mathbf{r}_d, \omega)$ is the (complex) degree of correlation. For simplicity, $S(-\mathbf{r}) = S(\mathbf{r})$ holds. To generate such a Schell-model correlation function, the generalized modes in Eq. (8) can be written as a Fourier-transform kernel,

$$\mathcal{A}(\mathbf{r}, \mathbf{v}) = S^{1/2}(\mathbf{r}) \exp(-2\pi i \mathbf{r} \cdot \mathbf{v}). \tag{11}$$

Inserting Eq. (11) into (8), we find that the potential correlation function can be written as

$$C(\mathbf{r}_1, \mathbf{r}_2, \omega) = [S(\mathbf{r}_1)S(\mathbf{r}_2)]^{1/2}\mathcal{F}[p(\mathbf{v})](\mathbf{r}_d), \tag{12}$$

where

$$\mathcal{F}[p(\mathbf{v})](\mathbf{r}_d) = \int p(\mathbf{v}) \exp(-2\pi i \mathbf{r}_d \cdot \mathbf{v}) d^3\mathbf{v} \tag{13}$$

is a 3D Fourier transform.

We assume the spectral density in the correlation function is a (very) slow function compared with the degree of correlation $F(\mathbf{r}_d)$; that is, the scatterer is quasihomogeneous [9]. Moreover, based on the convolution theorem, Eq. (12) can also be written in the form

$$C(\mathbf{r}_1, \mathbf{r}_2, \omega) = S(\mathbf{r}_s)[g(\mathbf{r}_d) \otimes g(\mathbf{r}_d)], \tag{14}$$

where $\mathbf{r}_s = (\mathbf{r}_1 + \mathbf{r}_2)/2$, $\otimes$ denotes the 3D convolution operation, and $g(\mathbf{r}_d) = \mathcal{F}[\sqrt{p(v)}](\mathbf{r}_d)$. Since $\sqrt{p(v)}$ is a real function, $g(\mathbf{r}_d)$ must satisfy the following condition:

$$g(-\mathbf{r}_d) = g^*(\mathbf{r}_d). \tag{15}$$

We find that the function $g(\mathbf{r}_d)$ obeys $\mathcal{PT}$ symmetry unless it is a real function. Thus, the potential correlation function for the Schell-model type calculated from Eq. (14) always has $\mathcal{PT}$ symmetry except the correlation function is real (classic symmetric).

B. Nonuniformly correlated type

The second example is the nonuniformly correlated potential correlation functions. In this case we express the generalized modes as

$$\mathcal{A}(\boldsymbol{\rho}, \mathbf{v}) = \exp\left[-\frac{(x^2 + y^2)}{\sigma_0^2}\right] \exp[-ia^n(x^n + y^n)] \times \exp\left[-iv\frac{(x^n + y^n)}{\xi_0^n}\right], \tag{16}$$

where $v = |\mathbf{v}|$, σ_0, a, ξ_0, and n are real-valued factors. The z dependence is not considered in the generalized modes since we have assumed the potential correlation function is uncorrelated along the z axis. We further take the spectral distribution function to be a circular Gaussian function, i.e.,

$$p(\mathbf{v}) = \sqrt{\frac{1}{2\pi}} \exp\left(-\frac{v^2}{2}\right). \tag{17}$$

Inserting Eqs. (16) and (17) into (8) and after integration, we find that the nonuniformly correlated potential correlation function can be expressed as

$$C(\mathbf{r}_1, \mathbf{r}_2, \omega) = \exp\left(-\frac{\boldsymbol{\rho}_1^2 + \boldsymbol{\rho}_2^2}{2\sigma_0^2}\right)\delta(z_1 - z_2) \times \exp\left[-\frac{\left[\left(x_1^n - x_2^n\right) + \left(y_1^n - y_2^n\right)\right]^2}{2\xi_0^{2n}}\right] \times \exp\left\{ia^n\left[\left(x_1^n - x_2^n\right) + \left(y_1^n - y_2^n\right)\right]\right\}. \tag{18}$$

From the above equation it is found that the parameter ξ_0 controls the spatial coherence width of the potential correlation function in the transverse plane, while the parameter a controls the strength of the second-order phase in the potential correlation function. We note that when the factor $a = 0$, the potential correlation function reduces to a real function and obeys the classic-symmetry condition. In addition, for $n = 1$, the potential correlation function takes on a Gaussian Schell-model form. Only when the factor $a \neq 0$ and the order n is an odd number does the nonuniformly correlated potential correlation function obey $\mathcal{PT}$ symmetry. When the order n is an even number, the correlation function becomes classic symmetric.

III. SCATTERING WITH $\mathcal{PT}$ RANDOM MEDIA

We assume that the random media discussed above are weak scatterers (i.e., the refractive index of the random medium differs only slightly from unity) and the scattering problem can be treated within the framework of the first-order Born approximation. The two-point cross-spectral density of the scattered field in the far field can be obtained by [9]

$$W^{\mathrm{s}}(r\mathbf{s}_1, r\mathbf{s}_2, \omega) = \frac{1}{r^2}\int_V\int_V W^{\mathrm{i}}(\mathbf{r}_1, \mathbf{r}_2, \omega)C(\mathbf{r}_1, \mathbf{r}_2, \omega) \times \exp[-ik(\mathbf{s}_2\cdot\mathbf{r}_2 - \mathbf{s}_1\cdot\mathbf{r}_1)]d^3\mathbf{r}_1 d^3\mathbf{r}_2, \tag{19}$$

where r is the distance from the scatterer to the far field, $\mathbf{s}_1$ and $\mathbf{s}_2$ are two directional unit vectors, $\int_V d^3\mathbf{r}$ denotes the integral over the 3D scatterer volume, and $W^{\mathrm{i}}(\mathbf{r}_1, \mathbf{r}_2, \omega)$ is the cross-spectral density of the incident light. We assume that the incident light is a polychromatic plane wave with its cross-spectral density written as

$$W^{\mathrm{i}}(\mathbf{r}_1, \mathbf{r}_2, \omega) = S(\omega)\exp[ik\mathbf{s}_0\cdot(\mathbf{r}_2 - \mathbf{r}_1)], \tag{20}$$

where $S(\omega)$ is the spectrum of the incident light and $\mathbf{s}_0$ is a unit vector representing the incident direction. For the normally incident light, $\mathbf{s}_0 = (0, 0, 1)$. Inserting Eqs. (10) and (20) into (19) and using $S^{\mathrm{s}}(r\mathbf{s}, \omega) = W^{\mathrm{s}}(r\mathbf{s}, r\mathbf{s}, \omega)$, we obtain the spectral density (or average intensity) of the far-zone scattered field,

$$S^{\mathrm{s}}(r\mathbf{s}_\perp, \omega) = \frac{S(\omega)}{r^2}\iint C(\boldsymbol{\rho}_1, \boldsymbol{\rho}_2, \omega) \times \exp[-i\mathbf{K}_\perp\cdot(\boldsymbol{\rho}_2 - \boldsymbol{\rho}_1)]d^2\boldsymbol{\rho}_1 d^2\boldsymbol{\rho}_2, \tag{21}$$

where $\mathbf{K}_\perp = k\mathbf{s}_\perp$, with $\mathbf{s}_\perp = (s_x, s_y)$ being the transverse unit vector. In the spherical coordinate frame, $s_x = \sin\theta\cos\phi$, and $s_y = \sin\theta\sin\phi$, where θ is the polar angle and ϕ is the azimuthal angle.

To check the symmetry property of the far-zone spectral density, we calculate the spectral density at the centrosymmetric position, i.e., at $-r\mathbf{s}_\perp$,

$$S^{\mathrm{s}}(-r\mathbf{s}_\perp, \omega) = \frac{S(\omega)}{r^2}\iint C(\boldsymbol{\rho}_1, \boldsymbol{\rho}_2, \omega) \times \exp[i\mathbf{K}_\perp\cdot(\boldsymbol{\rho}_2 - \boldsymbol{\rho}_1)]d^2\boldsymbol{\rho}_1 d^2\boldsymbol{\rho}_2. \tag{22}$$

The above equation can be modified into the form

$$S^{\mathrm{s}}(-r\mathbf{s}_\perp, \omega) = \frac{S(\omega)}{r^2}\iint C(-\boldsymbol{\rho}_1, -\boldsymbol{\rho}_2, \omega) \times \exp[-i\mathbf{K}_\perp\cdot(\boldsymbol{\rho}_2 - \boldsymbol{\rho}_1)]d^2\boldsymbol{\rho}_1 d^2\boldsymbol{\rho}_2. \tag{23}$$

On comparing Eqs. (21) and (23), we find that when $C(-\boldsymbol{\rho}_1, -\boldsymbol{\rho}_2, \omega) = C(\boldsymbol{\rho}_1, \boldsymbol{\rho}_2, \omega)$ (the condition for a classic-symmetric potential correlation function), the spectral density

$$S^{\mathrm{s}}(-r\mathbf{s}_\perp, \omega) = S^{\mathrm{s}}(r\mathbf{s}_\perp, \omega) \tag{24}$$

is centrosymmetric. However, for the $\mathcal{PT}$-symmetric potential correlation function this condition does not hold anymore. To see the symmetry structure of the spectral density induced by the $\mathcal{PT}$ random scatterer, we write the complex potential correlation function as

$$C(\boldsymbol{\rho}_1, \boldsymbol{\rho}_2, \omega) = C'(\boldsymbol{\rho}_1, \boldsymbol{\rho}_2, \omega) + iC''(\boldsymbol{\rho}_1, \boldsymbol{\rho}_2, \omega). \tag{25}$$

Thus, the spectral density in Eq. (21) can be split into

$$S^{\mathrm{s}}(r\mathbf{s}_\perp, \omega) = S^{\mathrm{s}\prime}(r\mathbf{s}_\perp, \omega) + iS^{\mathrm{s}\prime\prime}(r\mathbf{s}_\perp, \omega), \tag{26}$$

where $S^{\mathrm{s}\prime}(r\mathbf{s}_\perp, \omega)$ and $S^{\mathrm{s}\prime\prime}(r\mathbf{s}_\perp, \omega)$ are induced, respectively, by the real and imaginary parts of the correlation function. For the $\mathcal{PT}$-symmetric correlation, we have

$$C(-\boldsymbol{\rho}_1, -\boldsymbol{\rho}_2, \omega) = C'(\boldsymbol{\rho}_1, \boldsymbol{\rho}_2, \omega) - iC''(\boldsymbol{\rho}_1, \boldsymbol{\rho}_2, \omega). \tag{27}$$

Thus, the spectral density at $-r\mathbf{s}_\perp$ in Eq. (23) can be expressed as

$$S^{\mathrm{s}}(-r\mathbf{s}_\perp, \omega) = S^{\mathrm{s}\prime}(r\mathbf{s}_\perp, \omega) - iS^{\mathrm{s}\prime\prime}(r\mathbf{s}_\perp, \omega). \tag{28}$$

On comparing Eqs. (26) and (28), we obtain $S^{\mathrm{s}}(-r\mathbf{s}_\perp, \omega) \neq S^{\mathrm{s}}(r\mathbf{s}_\perp, \omega)$. The reason can be explained in the following way. Due to the spatially odd-symmetric distribution of the imaginary part of the refractive index for the potential realizations of the random scatterer, the (statistical) potential correlation function shows the same symmetry in its imaginary part. The far-field spectral density obtained by the Fourier transform of the potential correlation function [see Eq. (21)] thus becomes asymmetrical in the spatial domain. Thus, we can conclude that the spatial distribution of the far-zone spectral density of the scattered field from the normally incident plane-wave interaction with the $\mathcal{PT}$ random media is noncentrosymmetic.

IV. SIMULATION RESULTS

In this section, we show the simulation results of the spatial distribution of the far-zone spectral density generated by the light scattering with the classic-symmetric and $\mathcal{PT}$-symmetric random media whose potential correlation functions have Schell-model-correlated and nonuniformly correlated forms.

A. Schell-model potential correlations

The far-zone spectral density for a Schell-model potential correlation function can be calculated by inserting Eq. (14) into (21), i.e.,

$$S^{\mathrm{s}}(r\mathbf{s}_\perp, \omega) = \frac{S(\omega)}{r^2}\iint S(\boldsymbol{\rho}_s)[g(\boldsymbol{\rho}_d)\otimes g(\boldsymbol{\rho}_d)] \times \exp[-i\mathbf{K}_\perp\cdot\boldsymbol{\rho}_d]d^2\boldsymbol{\rho}_1 d^2\boldsymbol{\rho}_2, \tag{29}$$

where $\boldsymbol{\rho}_s = (\boldsymbol{\rho}_1 + \boldsymbol{\rho}_2)/2$ and $\boldsymbol{\rho}_d = \boldsymbol{\rho}_2 - \boldsymbol{\rho}_1$. With the help of the convolution theorem, Eq. (29) can be written as

$$S^{\mathrm{s}}(r\mathbf{s}_\perp, \omega) = \frac{S(\omega)\iint S(\boldsymbol{\rho}_s)d^2\boldsymbol{\rho}_s}{r^2}\{\mathcal{F}[g(\boldsymbol{\rho}_d)]\}^2. \tag{30}$$

Thus, the far-zone spectral density can be calculated by the traditional Fourier transform algorithm, e.g., fast-Fourier transform or chirp z-transform algorithms. In this work, we use the chirp z-transform algorithm to perform the Fourier transform in Eq. (30). The function $g(\boldsymbol{\rho}_d)$ is taken to be

$$g(\boldsymbol{\rho}_d) = \exp\left(-\frac{\boldsymbol{\rho}_d^2}{2\sigma_0^2}\right)\exp\left[-ia^n\left(x_d^n + y_d^n\right)\right], \tag{31}$$

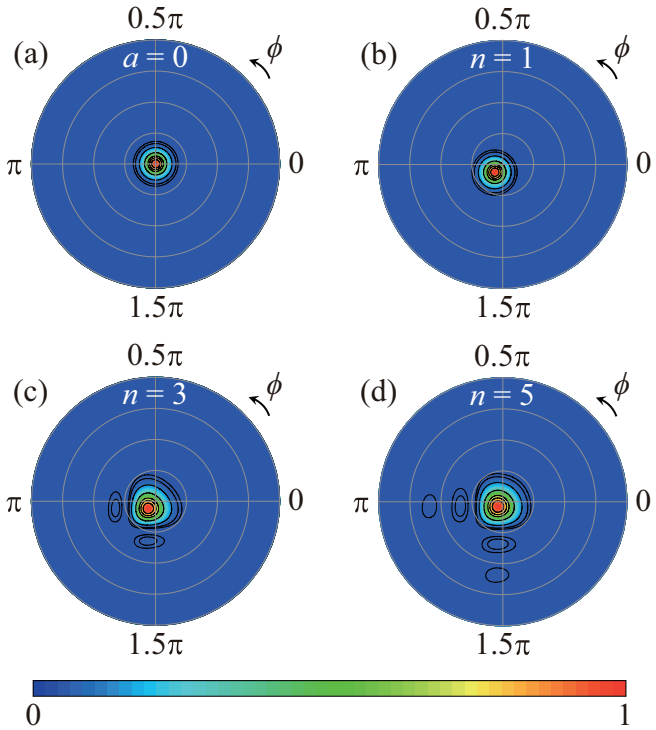

FIG. 1. Spatial distribution of the normalized far-zone spectral density generated by scattering a normally incident plane wave with a Schell-model-correlated random medium with the medium factor (a) $a = 0$, (b) $n = 1$, (c) $n = 3$, and (d) $n = 5$. In (b)–(d), $a = k/10$. In the simulation, $\sigma_0 = 10/k$, and the polar angle θ ranges from 0 to $\pi/2$.

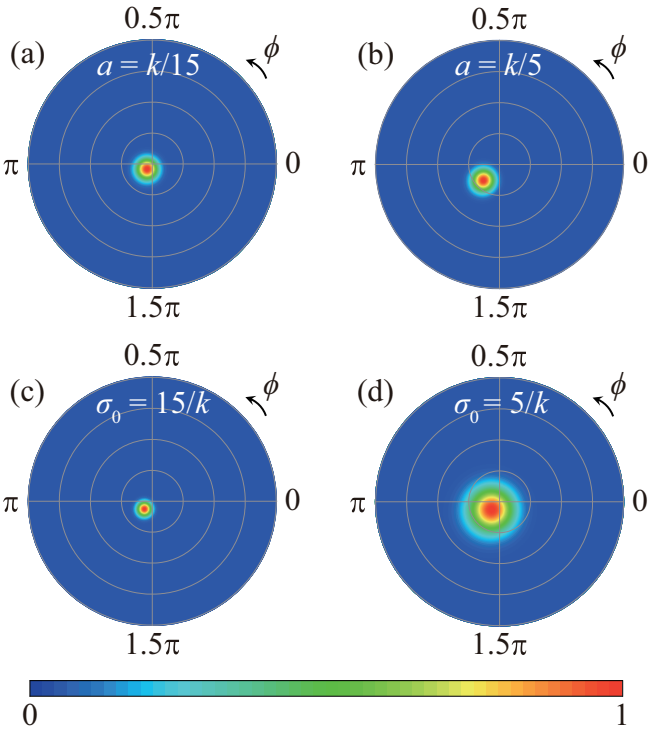

FIG. 2. Spatial distribution of the normalized far-zone spectral density generated by scattering a normally incident plane wave with a Schell-model-correlated random medium with the medium factor (a) $a = k/15$, (b) $a = k/5$, (c) $\sigma_0 = 15/k$, and (d) $\sigma_0 = 5/k$. In (a) and (b) $\sigma_0 = 10/k$, while in (c) and (d) $a = k/10$. In (a)–(d) $n = 1$, and the polar angle θ ranges from 0 to $\pi/2$.

where σ_0, a, and n are real factors. From Eq. (31), it is found that the factor σ_0 controls the spatial coherence width of the Schell-model potential correlations. We remark that when $a = 0$, the potential correlation function reduces to a (real) conventional Gaussian Schell-model function and thus has classic symmetry. For $a \neq 0$, the factor n must be an odd number to satisfy the condition in Eq. (15).

We display in Fig. 1 the far-zone spectral density of the scattered field generated by scattering a plane wave with the random media whose second-order potential correlation function is the Schell-model type. In Fig. 1(a), the factor $a = 0$, and thus, the potential correlation of the random scatterer obeys classic symmetry; we find the far-zone spectral density displays a Gaussian spot with centrosymmetric properties. However, when we let $a \neq 0$, the random media become $\mathcal{PT}$ symmetric. Thus, as shown in Figs. 1(b)–1(d), the spectral density in far field becomes noncentrosymmetric. With the increase of the value of n, the number of beamlets in the spectral density increases. We notice that the spatial distributions of the spectral density for $n = 3$ and $n = 5$ are similar to the intensity pattern of an Airy beam. This is due to the cubic phase (or higher-order odd-symmetric phase) in the potential correlation function.

To show the effect of the strength of the second-order phase and the spatial coherence width of the potential correlations on the far-field spectral density modulation, we plot in Fig. 2 the far-zone spectral density generated by scattering a normally incident plane wave with the Schell-model-correlated random media having different values of the factors a and σ_0. It is found from Figs. 2(a) and 2(b) as well as from Figs. 1(a) and 1(b) that with the increase of the strength (the value of a) of the second-order phase, the far-zone spectral density becomes more off axis or more noncentrosymmetric. This can be explained by the frequency-shifting property of a Fourier transform; that is, the phase shift in the potential correlation connects with the spatial shift of the spectral density in the far field. Figures 2(c), 2(d), and 1(b) show the effect of the spatial coherence width of the potential correlation function. We find that with the decrease of the spatial coherence, the beam spot for the far-zone spectral density expands because the self-interference effect in the random medium decreases. However, the off-axis distance of the beam spot is not changed since it depends only on the strength of the second-order phase. The even-symmetry property of the modulus of the potential correlation function does not affect the off-axis distance of the beam spot.

B. Nonuniformly correlated potential correlations

The far-zone spectral density of the nonuniformly correlated random media can be calculated numerically in the following way. We first approximate $p(v)$ in Eq. (17) by a discrete set $\{p_m\}$ of weights at sampled points $\{v_m\}$,

$$p(v) \simeq \sum_{m=0}^{M-1} p_m \delta(v - v_m), \tag{32}$$

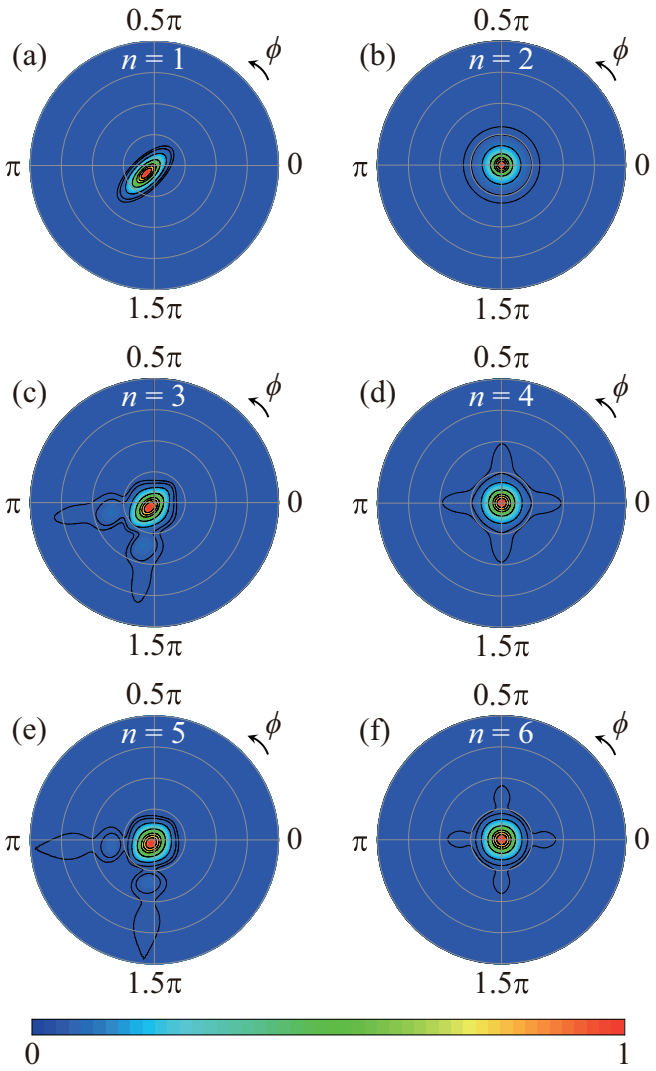

FIG. 3. Spatial distribution of the normalized far-zone spectral density generated by scattering a normally incident plane wave with a nonuniformly correlated random medium with the medium factor (a) $n = 1$, (b) $n = 2$, (c) $n = 3$, (d) $n = 4$, (e) $n = 5$, and (f) $n = 6$. In the simulation, $\sigma_0 = \xi_0 = 10/k$, $a = k/10$, and the polar angle θ ranges from 0 to $\pi/2$.

where M is the number of sampling points. The potential correlation function thus can be expressed in the form of pseudomode representation,

$$C(\boldsymbol{\rho}_1, \boldsymbol{\rho}_2, \omega) \simeq \sum_{m=0}^{M-1} p_m \mathcal{A}^*(\boldsymbol{\rho}_1, v_m)\mathcal{A}(\boldsymbol{\rho}_2, v_m). \tag{33}$$

Inserting Eq. (33) into (21), we find that the far-zone spectral density can be calculated by

$$S^{\mathrm{s}}(r\mathbf{s}_\perp, \omega) \simeq \frac{S(\omega)}{r^2} \sum_{m=0}^{M-1} p_m |\mathcal{F}[\mathcal{A}(\boldsymbol{\rho}, v_m)]|^2. \tag{34}$$

Since $p(v)$ is a circular Gaussian function, we can safely assume that $v_m \leqslant v_{\max} = 3$ in our numerical calculation. In Fig. 3, we display the far-zone spectral density generated by

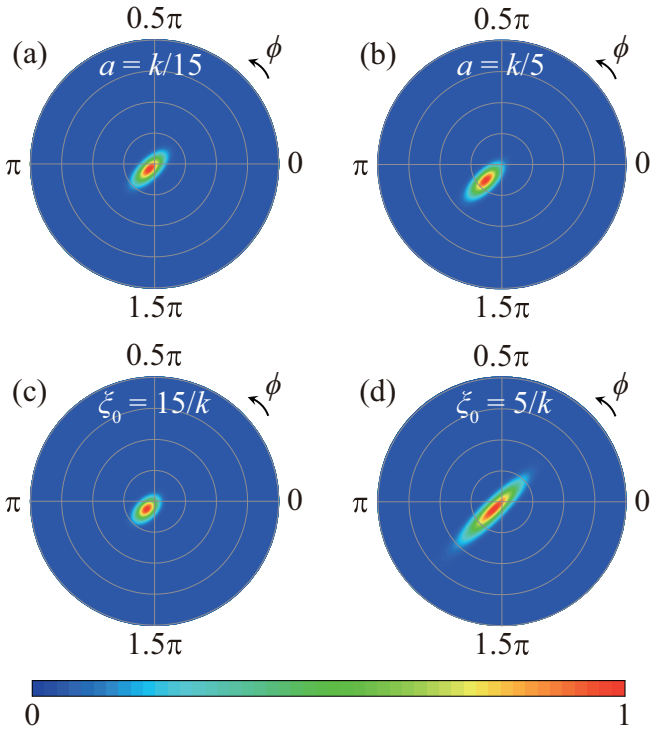

FIG. 4. Spatial distribution of the normalized far-zone spectral density generated by scattering a normally incident plane wave with a nonuniformly correlated random medium with the medium factor (a) $a = k/15$, (b) $a = k/5$, (c) $\xi_0 = 15/k$, and (d) $\xi_0 = 5/k$. In (a) and (b) $\xi_0 = 10/k$, while in (c) and (d) $a = k/10$. In (a)–(d) $n = 1$, $\sigma_0 = 10/k$, and the polar angle θ ranges from 0 to $\pi/2$.

scattering a plane wave with nonuniformly correlated random media with different medium orders n. As we discussed above, when the factor n is an odd number, the potential correlation function obeys $\mathcal{PT}$ symmetry. Thus, the far-zone spectral density, as shown in the left column of Fig. 3, is noncentrosymmetric. However, when n is an even number, the potential correlation function becomes classic symmetric, and therefore, the induced spectral density in the far field become centrosymmetric (right column of Fig. 3).

The effects of the phase strength and the spatial coherence width of the nonuniformly correlated potential correlation on the far-zone spectral density are shown in Fig. 4. Effects similar to those of the Schell-model potential correlations are found. With the increase of the phase strength, we find in Figs. 4(a), 4(b), and 3(a) that the off-axis distance increases, and with the decrease of the spatial coherence width of the random potential the beam spot expands in the far-zone spectral density distribution.

V. CONCLUSIONS

In summary, based on the weak-potential-scattering theory and the theory for optical coherence, we examined the far-zone spectral density of a plane wave scattered by random media with the second-order potential correlation function obeying $\mathcal{PT}$ symmetry. Both Schell-model-correlated and nonuniformly correlated types of potential correlations were considered for the random media. We showed that the

random media with complex Schell-model-correlated correlations always obey $\mathcal{PT}$ symmetry due to the non-negative condition for the correlation function. However, for the nonuniformly correlated random media, the potential correlation function has $\mathcal{PT}$ symmetry only when its phase displays an odd-symmetric distribution. When the potential correlation function is real or for the even-symmetric phase distribution, the random media obey the classic symmetry. We showed both analytically and numerically that $\mathcal{PT}$ symmetry in the potential correlation function breaks the centrosymmetry of the spectral density of the far-zone scattered field. The high-even-order phase in the potential correlation functions can induce Airy-like patterns. We showed that with the increase of the second-order phase strength, the far-zone scattered field becomes more noncentrosymmetric. In contrast, with the decrease of the spatial coherence width of the potential correlation function, the beam spot in the far field expands without changing the off-axis distance.

Finally, our work revealed a different way to control the symmetry property of the scattered field by modifying the potential correlation function of the random scatterer into $\mathcal{PT}$ or classic symmetry. We anticipate that the far-zone asymmetry spectral density (and two-point correlation function) measurement can be used for inversely recovering the intrinsic symmetry feature of a random scatterer. We notice that in a recent work by Korotkova and Brandão, the general coherence theory for the light source with $\mathcal{PT}$ symmetry was introduced [72]. Thus, we expect that the asymmetry distribution of the far-zone scattered field can be enhanced or suppressed by the joint effect from the $\mathcal{PT}$ symmetry of the incident light and random media. This work can be extended into the vectorial case to analyze the asymmetry distribution of the polarization state in scattered fields with the help of the electromagnetic coherence theory [8,29].

ACKNOWLEDGMENTS

This research was supported by the National Key Research and Development Project of China (2019YFA0705000), the National Natural Science Foundation of China (NSFC) (91750201, 11874046, 11974218, 11904247, and 12192254), the Innovation Group of Jinan (2018GXRC010), and the Local Science and Technology Development Project of the Central Government (No. YDZX20203700001766).

[1] M. Born and E. Wolf, *Principles of Optics* (Cambridge University Press, Cambridge, 1999).
[2] A. Ishimaru, *Wave Propagation and Scattering in Random Media* (Academic Press, New York, 1978).
[3] O. M. Maragò, P. H. Jones, P. G. Gucciardi, G. Volpe, and A. C. Ferrari, Optical trapping and manipulation of nanostructures, Nat. Nanotechnol. **8**, 807 (2013).
[4] D. Paganin, *Coherent X-Ray Optics* (Oxford University Press, Oxford, 2006).
[5] L. C. Andrews and R. L. Phillips, *Laser Beam Propagation Through Random Medium*, 2nd ed. (SPIE, Bellinghan, 2005).
[6] L. Mandel and E. Wolf, *Optical Coherence and Quantum Optics* (Cambridge University Press, Cambridge, 1995).
[7] A. Dogariu and R. Carminati, Electromagnetic field correlations in three-dimensional speckles, Phys. Rep. **559**, 1 (2015).
[8] A. T. Friberg and T. Setälä, Electromagnetic theory of optical coherence (invited), J. Opt. Soc. Am. A **33**, 2431 (2016).
[9] E. Wolf, *Introduction to the Theory of Coherence and Polarization of Light* (Cambridge University Press, Cambridge, 2007).
[10] D. Cabaret, S. Rossano, and C. Brouder, Mie scattering of a partially coherent beam, Opt. Commun. **150**, 239 (1998).
[11] J.-J. Greffet, M. D. L. Cruz-Gutierrez, P. V. Ignatovich, and A. Radunsky, Influence of spatial coherence on scattering by a particle, J. Opt. Soc. Am. A **20**, 2315 (2003).
[12] T. van Dijk, D. G. Fischer, T. D. Visser, and E. Wolf, Effects of Spatial Coherence on the Angular Distribution of Radiant Intensity Generated by Scattering on a Sphere, Phys. Rev. Lett. **104**, 173902 (2010).
[13] H. F. Schouten, D. G. Fischer, and T. D. Visser, Coherence modification and phase singularities on scattering by a sphere: Mie formulation, J. Opt. Soc. Am. A **36**, 2005 (2019).
[14] J. Liu, L. Bi, P. Yang, and G. W. Kattawar, Scattering of partially coherent electromagnetic beams by water droplets and ice crystals, J. Quantum Spectrosc. Radiat. Transfer **134**, 74 (2014).
[15] S. Sukhov, D. Haefner, J. Bae, D. Ma, D. R. Carter, and A. Dogariu, Effect of spatial coherence on scattering from optically inhomogeneous media, J. Opt. Soc. Am. A **29**, 85 (2012)
[16] J. Lindberg, T. T. Setälä, M. Kaivola, and A. T. Friberg, Spatial coherence effects in light scattering from metallic nanocylinders, J. Opt. Soc. Am. A **23**, 1349 (2006).
[17] Y. Liu and X. Zhang, Coherent effect in superscattering, J. Opt. Soc. Am. A **33**, 2071 (2016).
[18] T. Saastamoinen and H. Lajunen, Increase of spatial coherence by subwavelength metallic gratings, Opt. Lett. **38**, 5000 (2013).
[19] Y. Wang, H. F. Schouten, and T. D. Visser, Tunable, anomalous Mie scattering using spatial coherence, Opt. Lett. **40**, 4779 (2015).
[20] Y. Wang, D. Kuebel, T. D. Visser, and E. Wolf, Creating von Laue patterns in crystal scattering with partially coherent sources, Phys. Rev. A **94**, 033812 (2016).
[21] S. Ponomarenko, J. J. Greffet, and E. Wolf, The diffusion of partially coherent beams in turbulent media, Opt. Commun. **208**, 1 (2002).
[22] L. E. Estes, L. M. Narducci, and R. A. Tuft, Scattering of light from a rotating ground glass, J. Opt. Soc. Am. **61**, 1301 (1971).
[23] L. G. Cançado, R. Beams, A. Jorio, and L. Novotny, Theory of Spatial Coherence in Near-Field Raman Scattering, Phys. Rev. X **4**, 031054 (2014).
[24] R. Beams, L. G. Cançado, S.-H. Oh, A. Jorio, and L. Novotny, Spatial Coherence in Near-Field Raman Scattering, Phys. Rev. Lett. **113**, 186101 (2014).
[25] D. Zhao and T. Wang, Direct and inverse problem in the theory of light scattering, Prog. Opt. **57**, 261 (2012).

[26] W. H. Carter and E. Wolf, Scattering from quasi-homogeneous media, Opt. Commun. **67**, 85 (1988).

[27] E. Wolf, Far-zone spectral isotropy in weak scattering on spatially random media, J. Opt. Soc. Am. A **14**, 2820 (1997).

[28] T. D. Visser, D. G. Fischer, and E. Wolf, Scattering of light from quasi-homogeneous sources by quasi-homogeneous media, J. Opt. Soc. Am. A **23**, 1631 (2006).

[29] Z. Tong and O. Korotkova, Theory of weak scattering of stochastic electromagnetic fields from deterministic and random media, Phys. Rev. A **82**, 033836 (2010).

[30] Y. Wang, S. Yan, D. Kuebel, and T. D. Visser, Dynamic control of light scattering using spatial coherence, Phys. Rev. A **92**, 013806 (2015).

[31] D. G. Fischer and E. Wolf, Inverse problems with quasi-homogeneous media, J. Opt. Soc. Am. A **11**, 1128 (1994).

[32] D. Zhao, O. Korotkova, and E. Wolf, Application of correlation-induced spectral changes to inverse scattering, Opt. Lett. **32**, 3483 (2007).

[33] M. Lahiri, E. Wolf, D. G. Fischer, and T. Shirai, Determination of Correlation Functions of Scattering Potentials of Stochastic Media from Scattering Experiments, Phys. Rev. Lett. **102**, 123901 (2009).

[34] O. Korotkova, Design of weak scattering media for controllable light scattering, Opt. Lett. **40**, 284 (2015).

[35] O. Korotkova, Can a sphere scatter light producing rectangular intensity patterns? Opt. Lett. **40**, 1709 (2015).

[36] P. A. Brandão and O. Korotkova, Scattering theory for stationary materials with $\mathcal{PT}$ symmetry, Phys. Rev. A **103**, 013502 (2021).

[37] C. M. Bender and S. Boettcher, Real Spectra in Non-Hermitian Hamiltonians Having $\mathcal{PT}$ symmetry, Phys. Rev. Lett. **80**, 5243 (1998).

[38] C. M. Bender, Making sense of non-Hermitian Hamiltonians, Rep. Prog. Phys. **70**, 947 (2007).

[39] C. E. Rüter, K. G. Makris, R. El-Ganainy, D. N. Christodoulides, M. Segev, and D. Kip, Observation of parity-time symmetry in optics, Nat. Phys. **6**, 192 (2010).

[40] L. Feng, R. El-Ganainy, and L. Ge, Non-Hermitian photonics based on parity-time symmetry, Nat. Photonics **11**, 752 (2017).

[41] Z. Lin, H. Ramezani, T. Eichelkraut, T. Kottos, H. Cao, and D. N. Christodoulides, Unidirectional Invisibility Induced by $\mathcal{PT}$-Symmetric Periodic Structures, Phys. Rev. Lett. **106**, 213901 (2011).

[42] L. Ge, Y. Chong, and A. D. Stone, Conservation relations and anisotropic transmission resonances in one-dimensional $\mathcal{PT}$-symmetric photonic heterostructures, Phys. Rev. A **85**, 023802 (2012).

[43] L. Feng, Y.-L. Xu, W. S. Fegadolli, M.-H. Lu, J. E. Oliveira, V. R. Almeida, Y.-F. Chen, and A. Scherer, Experimental demonstration of a unidirectional reflectionless parity-time metamaterial at optical frequencies, Nat. Mater. **12**, 108 (2013).

[44] J. Wiersig, Enhancing the Sensitivity of Frequency and Energy Splitting Detection by Using Exceptional Points: Application to Microcavity Sensors for Single-Particle Detection, Phys. Rev. Lett. **112**, 203901 (2014).

[45] P. Miao, Z. Zhang, J. Sun, W. Walasik, S. Longhi, N. M. Litchinitser, and L. Feng, Orbital angular momentum microlaser, Science **353**, 464 (2016).

[46] I. V. Doronin, A. A. Zyablovsky, E. S. Andrianov, A. A. Pukhov, and A. P. Vinogradov, Lasing without inversion due to parametric instability of the laser near the exceptional point, Phys. Rev. A **100**, 021801(R) (2019).

[47] S. Assawaworrarit, X. Yu, and S. Fan, Robust wireless power transfer using a nonlinear parity-time-symmetric circuit, Nature (London) **546**, 387 (2017).

[48] S. Weimann, M. Kremer, Y. Plotnik, Y. Lumer, S. Nolte, K. G. Makris, M. Segev, M. C. Rechtsman, and A. Szameit, Topologically protected bound states in photonic parity-time-symmetric crystals, Nat. Mater. **16**, 433 (2017).

[49] P. A. Brandão and S. B. Cavalcanti, Scattering of partially coherent radiation by non-Hermitian localized structures having parity-time symmetry, Phys. Rev. A **100**, 043822 (2019).

[50] D. G. Pires, N. M. Litchinitser, and P. A. Brandão, Scattering of partially coherent vortex beams by a PT-symmetric dipole, Opt. Express **29**, 15576 (2021).

[51] M. A. Pinto and P. A. Brandão, Asymmetrical splitting in the spectrum of stochastic radiation scattered by non-Hermitian materials having $\mathcal{PT}$ symmetry, Phys. Rev. A **101**, 053817 (2020).

[52] P. A. Brandão and S. B. Cavalcanti, Non-Hermitian spectral changes in the scattering of partially coherent radiation by periodic structures, Opt. Lett. **44**, 4363 (2020).

[53] O. Korotkova and P. A. Brandão, Light scattering from stationary PT-symmetric collections of particles, Opt. Lett. **46**, 1417 (2021).

[54] A. Lubatsch, J. Kroha, and K. Busch, Theory of light diffusion in disordered media with linear absorption or gain, Phys. Rev. B **71**, 184201 (2005).

[55] R. Frank, A. Lubatsch, and J. Kroha, Theory of strong localization effects of light in disordered loss or gain media, Phys. Rev. B **73**, 245107 (2006).

[56] R. Frank and A. Lubatsch, Scalar wave propagation in random amplifying media: Influence of localization effects on length and time scales and threshold behavior, Phys. Rev. A **84**, 013814 (2011).

[57] A. Lubatsch and R. Frank, Tuning the quantum efficiency of random lasers - intrinsic stokes-shift and gain, Sci. Rep. **5**, 17000 (2015).

[58] A. Lubatsch and R. Frank, A self-consistent quantum field theory for random lasing, Appl. Sci. **9**, 2477 (2019).

[59] A. Lubatsch and R. Frank, Self-consistent quantum field theory for the characterization of complex random media by short laser pulses, Phys. Rev. Research **2**, 013324 (2020).

[60] H. Li, S. Yin, E. Galiffi, and A. Alù, Temporal Parity-Time Symmetry for Extreme Energy Transformations, Phys. Rev. Lett. **127**, 153903 (2021).

[61] A. Lagendijk, B. van Tiggelen, and D. Wiersma, Notes on Anderson localization, Phys. Today **65**(5), 11 (2012).

[62] T. Sperling, W. Bührer, C. M. Aegerter, and G. Maret, Direct determination of the transition to localization of light in three dimensions, Nat. Photonics **7**, 48 (2013).

[63] F. Scheffold and D. Wiersma, Inelastic scattering puts in question recent claims of Anderson localization of light, Nat. Photonics **7**, 934 (2013).

[64] G. Maret, T. Sperling, W. Bührer, A. Lubatsch, R. Frank, and C. M. Aegerter, Inelastic scattering puts in question recent claims of Anderson localization of light, Nat. Photonics **7**, 934 (2013).

[65] C. Conti and A. Fratalocchi, Dynamic light diffusion, three-dimensional Anderson localization and lasing in inverted opals, Nat. Phys. **4**, 794 (2008).

[66] B. H. Hokr, J. N. Bixler, M. T. Cone, J. D. Mason, H. T. Beier, G. D. Noojin, G. I. Petrov, L. A. Golovan, R. J. Thomas, B. A. Rockwell, and V. V. Yakovlev, Bright emission from a random Raman laser, Nat. Commun. **5**, 4356 (2014).

[67] M. Bellingeri, A. Chiasera, I. Kriegel, and F. Scotognella, Optical properties of periodic, quasi-periodic, and disordered one-dimensional photonic structures, Opt. Mater. **72**, 403 (2017).

[68] S. Rotter and S. Gigan, Light fields in complex media: Mesoscopic scattering meets wave control, Rev. Mod. Phys. **89**, 015005 (2017).

[69] E. G. Kostadinova, J. L. Padgett, C. D. Liaw, L. S. Matthews, and T. W. Hyde, Numerical study of anomalous diffusion of light in semicrystalline polymer structures, Phys. Rev. Research **2**, 043375 (2020).

[70] R. Kolkowski, S. Kovaios, and A. F. Koenderink, Pseudochirality at exceptional rings of optical metasurfaces, Phys. Rev. Research **3**, 023185 (2021).

[71] S. Yu, C.-W. Qiu, Y. Chong, S. Torquato, and N. Park, Engineered disorder in photonics, Nat. Rev. Mater. **6**, 226 (2021).

[72] O. Korotkova and P. A. Brandão, Coherence theory for electromagnetic, planar, PT-symmetric light sources, Opt. Lett. **46**, 3576 (2021).